Electronic supplementary Information:

3D/2D Bi_2S_3/SnS_2 Heterostructures: Superior Charge Separation and Enhanced Solar Light Driven Photocatalytic Performance

Sumana Paul[1,3†], Dulal Barman[1⁋†], Chandra Chowdhury[2], P. K. Giri[3] and Subodh Kumar De[1*]

[1]*Scool of Materials Sciences, Indian Association for the Cultivation of Science, Jadavpur, Kolkata- 700032, India*

[2]*Institute of Catalysis Research and Technology (IKFT), Karlsruhe Institute of Technology (KIT), Eggenstein-Leopoldshafen, Germany.*

[3]*Department of Physics, Indian Institute of Technology Guwahati, Guwahati 781039, India.*

*E-mail: msskd@iacs.res.in

†Authors Contributed Equally

⁋ Present Address: Department of Physics, Balurghat College, Balurghat, Dakshin Dinajpur 733101, India.

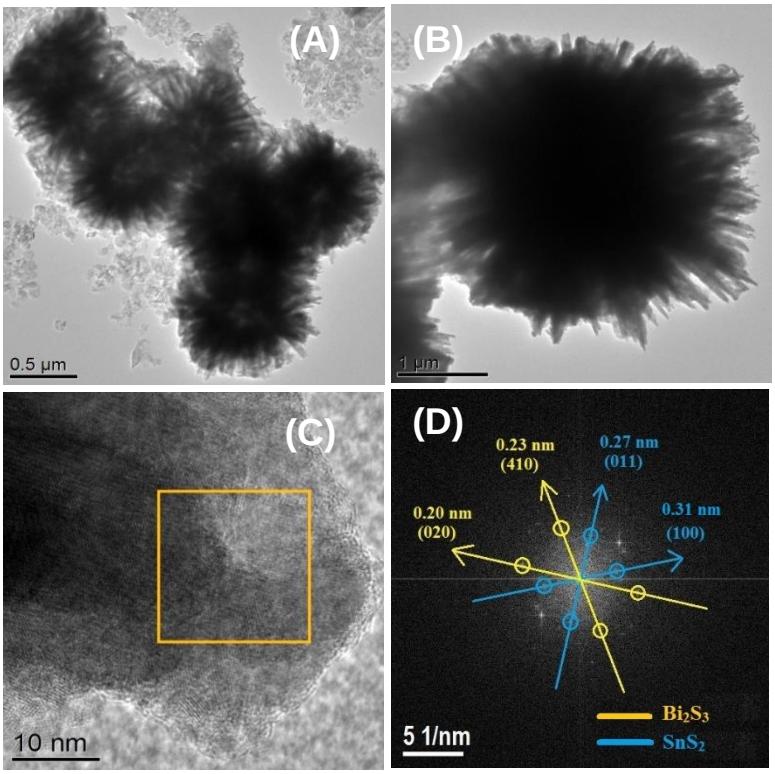

Fig. S1. (A) TEM image of BSS2 heterostructure. (B) A closer view of densely SnS_2 decorated Bi_2S_3 urchine. (C) HRTEM image of a nanorod fully covered with SnS_2 nanosheets. (D) FFT pattern obtained from the yellow square region showing planes of both Bi_2S_3 and SnS_2 where (011), (210) correspond of planes Bi_2S_3 and (012), (001) corresponds to planes of SnS_2.

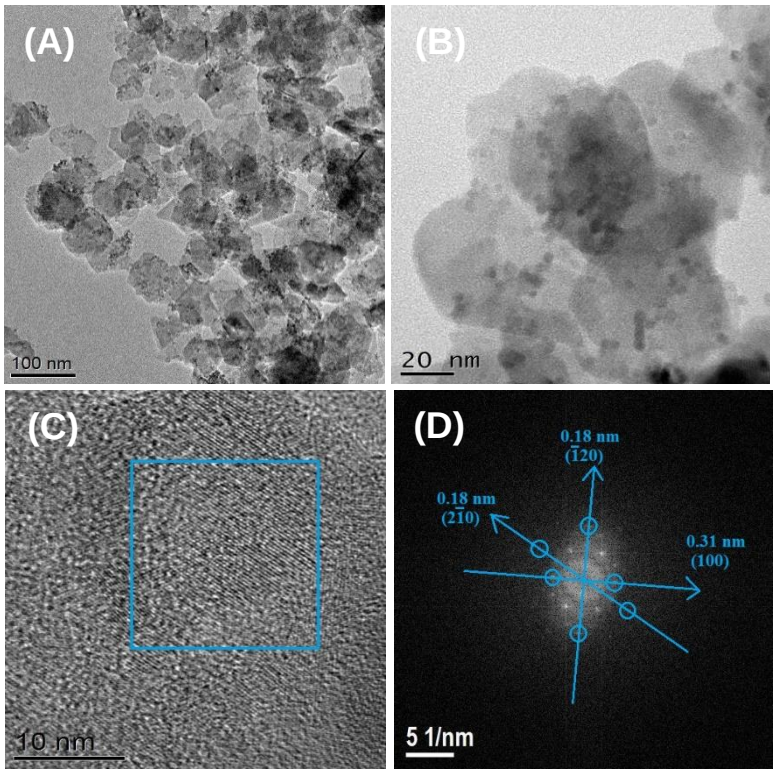

Fig. S2. (A) Large area TEM image of SnS_2 nanosheets. (B) A closer view of a few nanosheets. (C) HRTEM image obtained from a single SnS_2 nanosheet. (D) FFT pattern obtained from the blue square region showing the planes (100), $(1\bar{2}0)$, $(21\bar{0})$ of SnS_2.

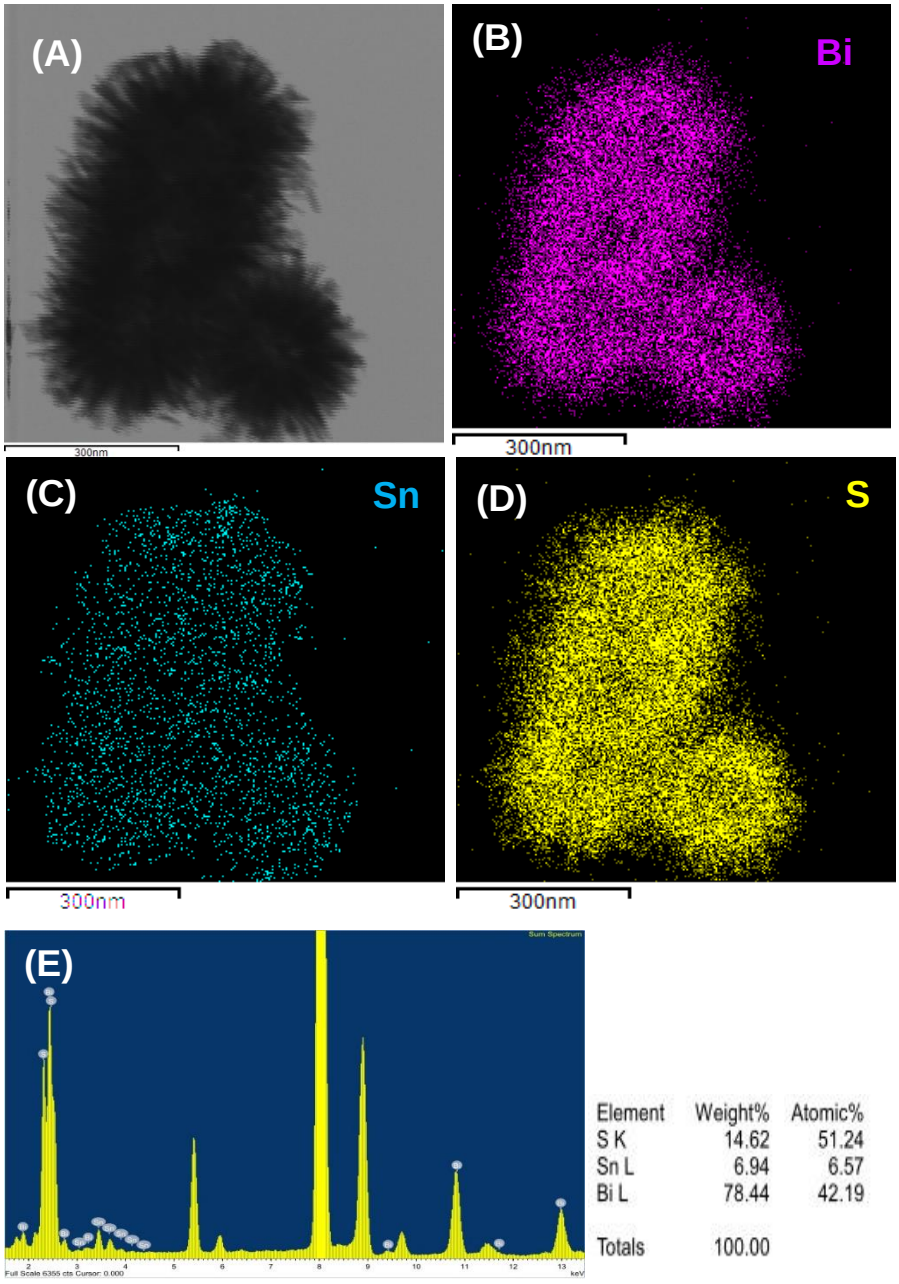

Fig. S3. TEM image (A) of the Bi_2S_3/SnS_2 heterostructure (BSS1.5) and the corresponding EDS mapping of Bi (B, magenta), Sn (C, cyan) and S (D, yellow) and (E) the EDS scan.

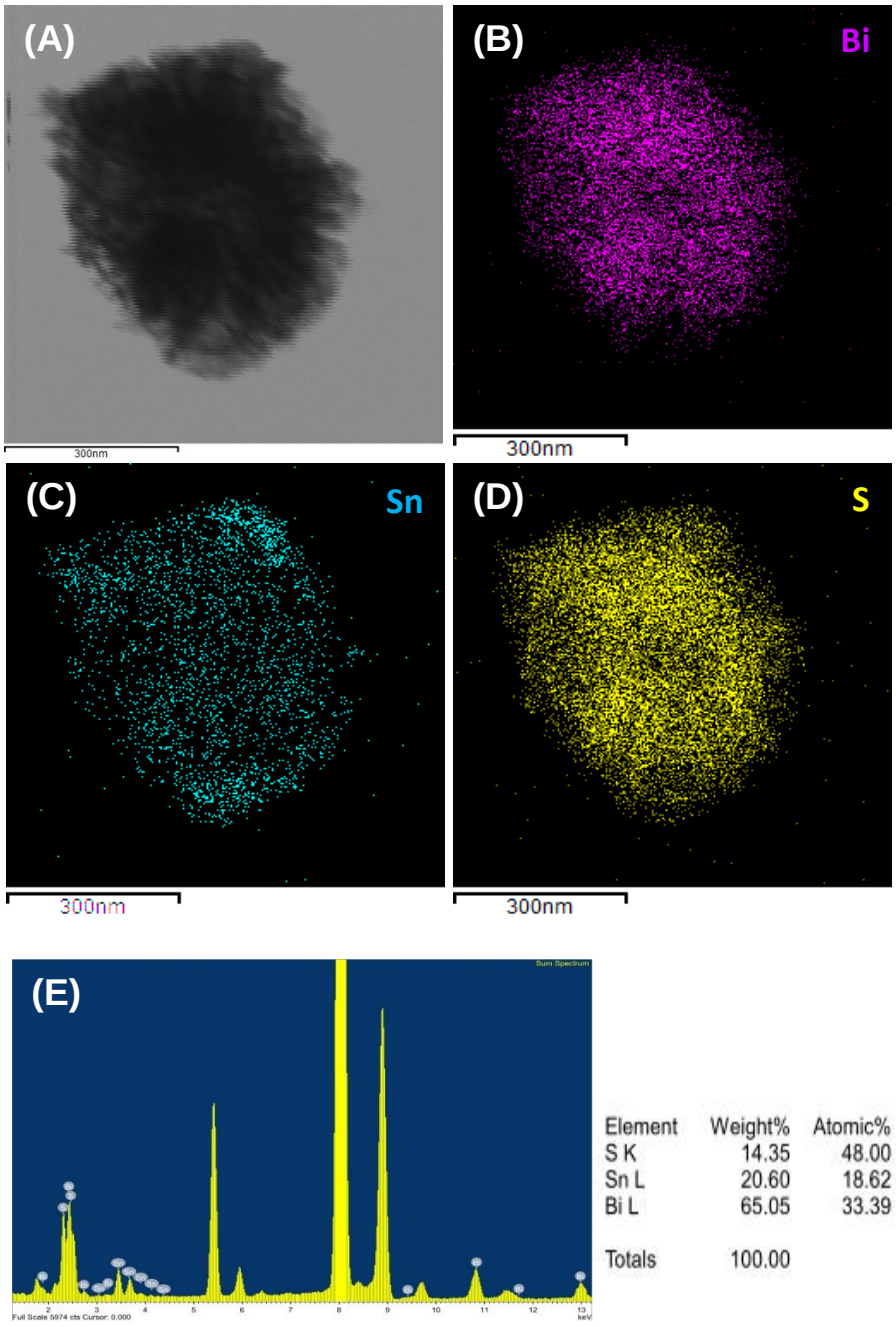

Fig. S4. TEM image (A) of the Bi_2S_3/SnS_2 heterostructure (BSS2) and the corresponding EDS mapping of Bi (B, magenta), Sn (C, cyan) and S (D, yellow) and (E) the EDS scan.

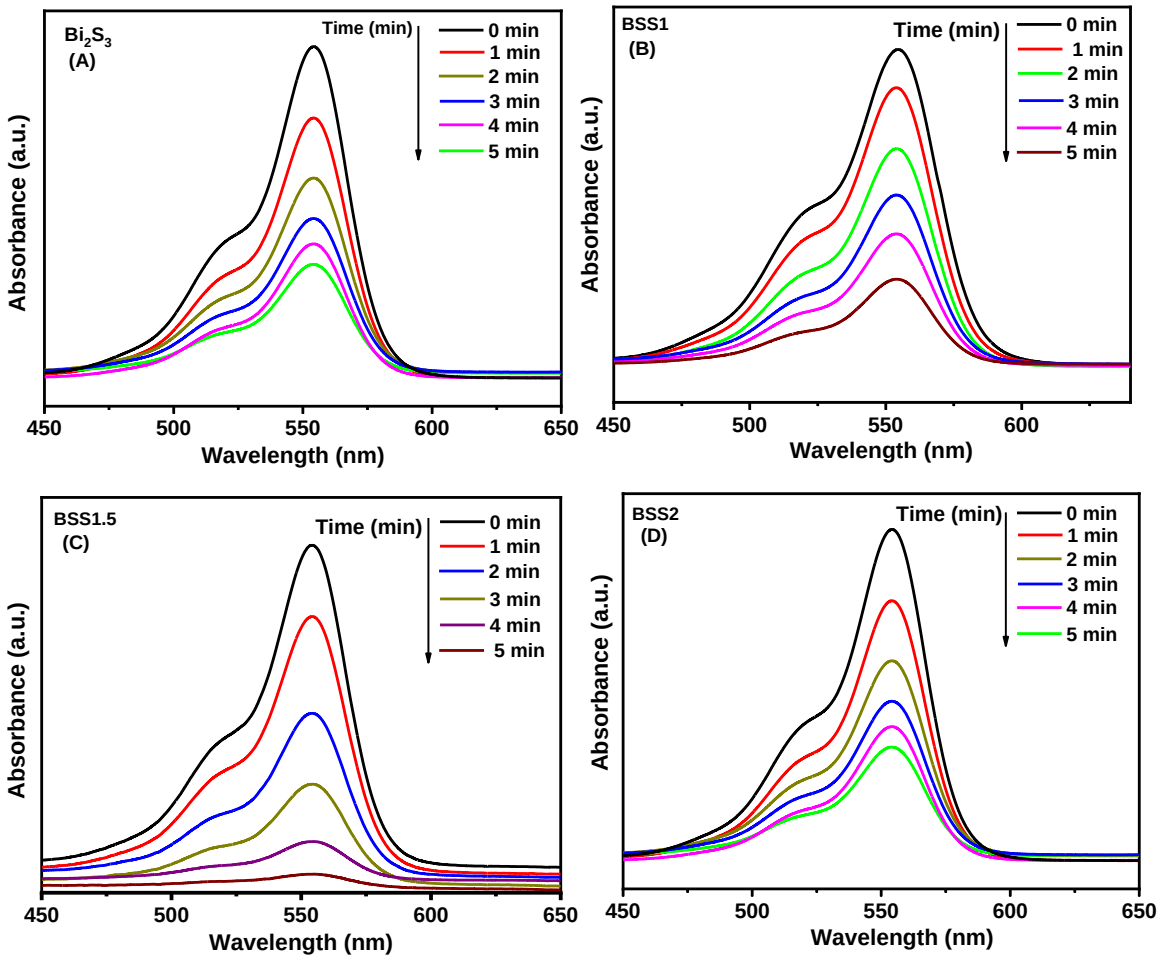

Fig. S5. Photocatalytic degradation of RhB dye in presence of (A) Bi_2S_3 urchines, (B) BSS1, (C) BSS1.5 and (D) BSS2 heterostructure under solar simulator.

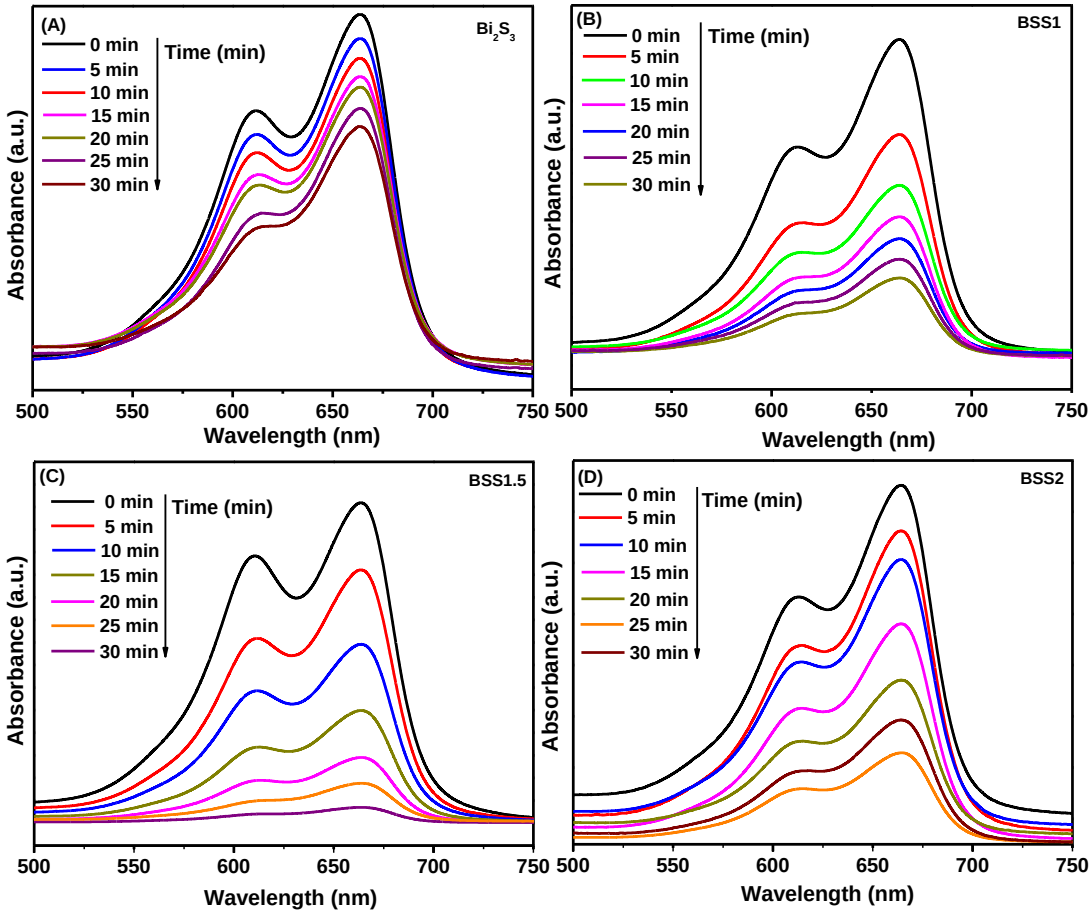

Fig. S6. Photocatalytic degradation of MB dye in presence of (A) Bi_2S_3 urchines, (B) BSS1, (C) BSS1.5 and (D) BSS2 heterostructures under solar simulator.

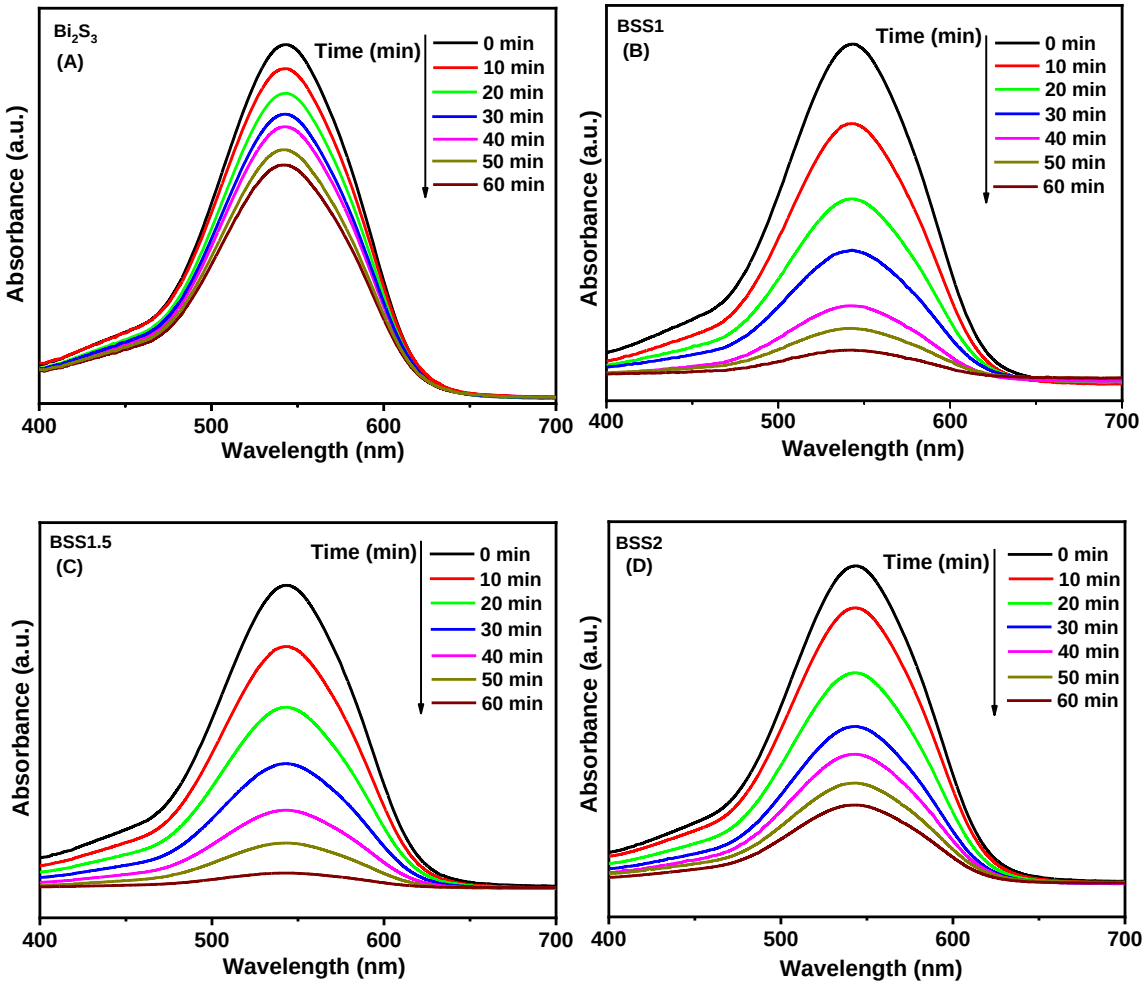

Fig. S7. Detection of Cr(VI) in presence of (A) Bi_2S_3 urchines, (B) BSS1, (C) BSS1.5 and (D) BSS2 heterostructure under solar simulator.

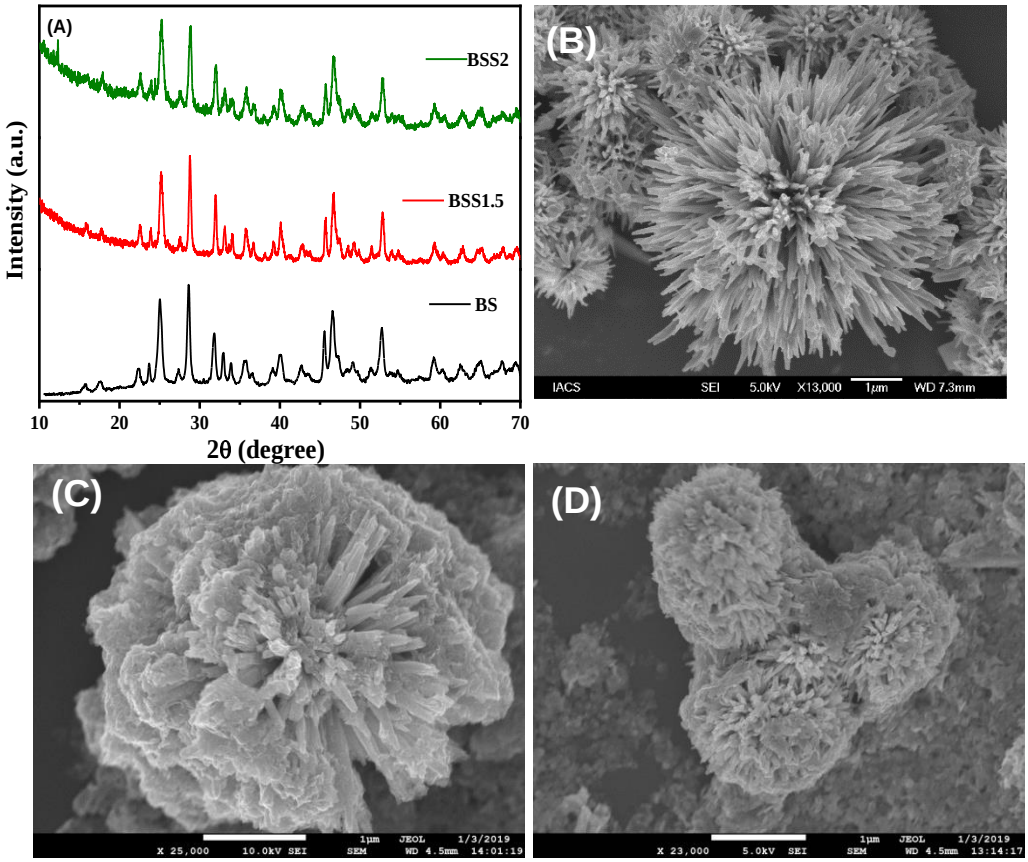

Fig. S8. XRD pattern of (A) pure Bi_2S_3, BSS1.5 and BSS2 heterostructures after photocatalytic activity and SEM images of (B) pure Bi_2S_3, (C) BSS1.5 and (D) BSS2 heterostructures after photocatalytic activity.

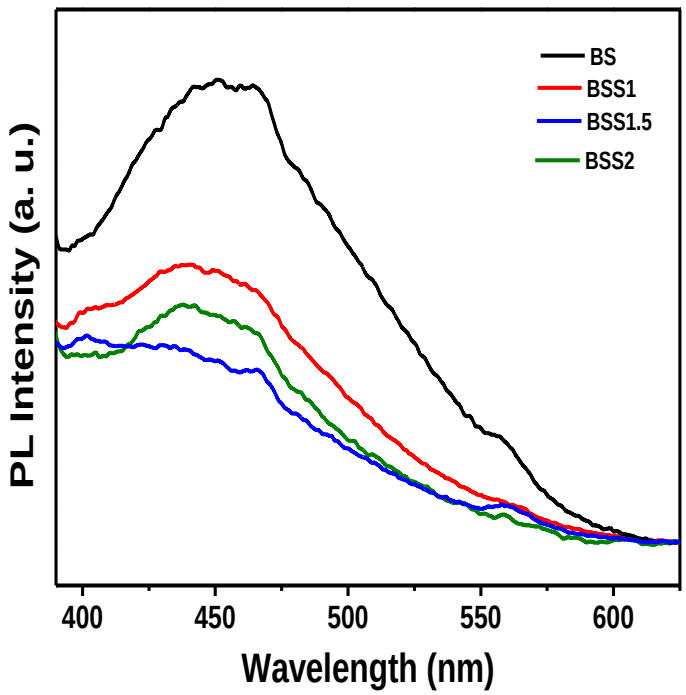

Fig. S9. Room temperature PL spectra of different photocatalysts.

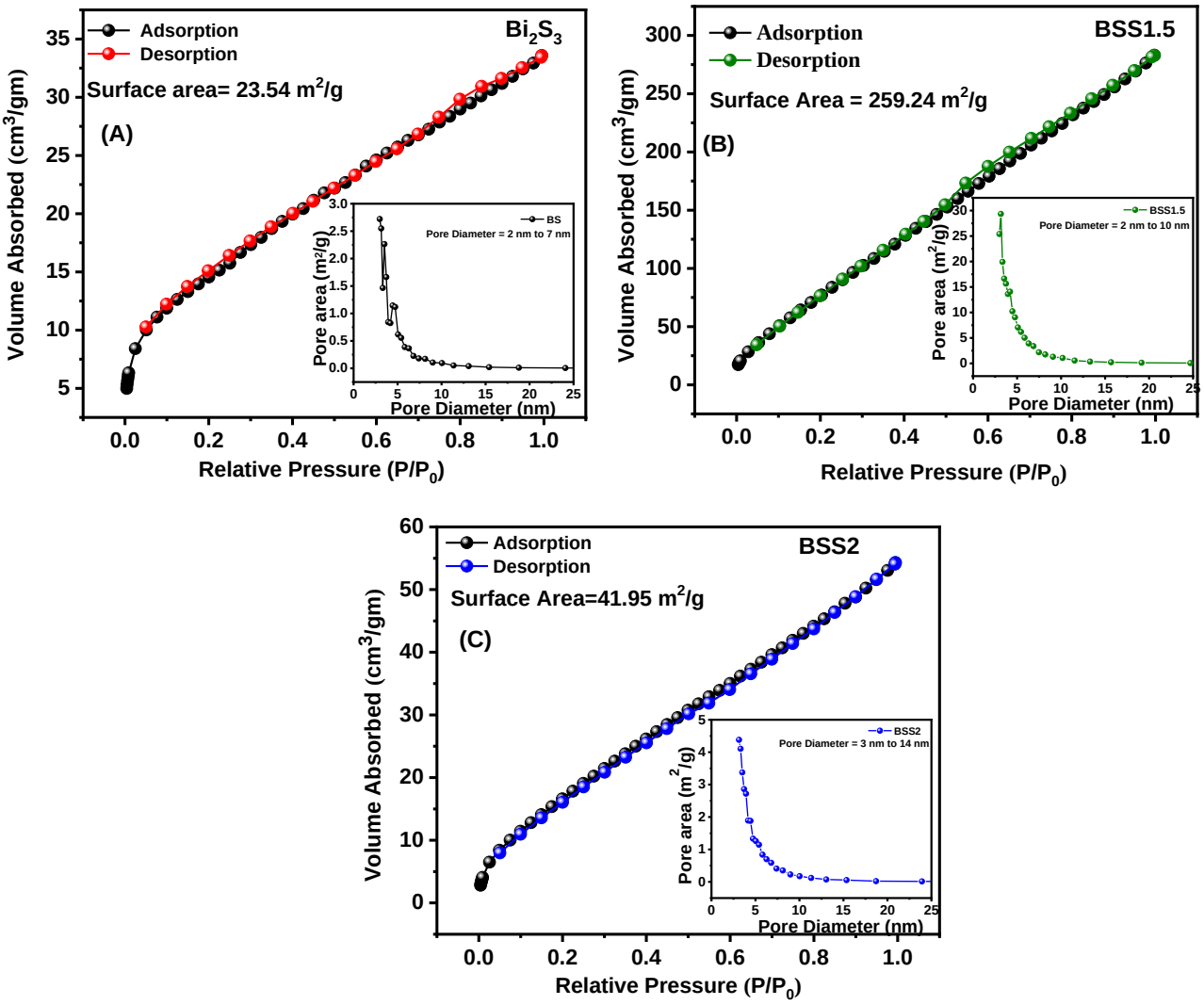

Fig. S10. BET adsorption–desorption isotherms and the pore-size distribution (inset) of (A) pure Bi_2S_3, (B) BSS1.5 and (C) BSS2 heterostructures.

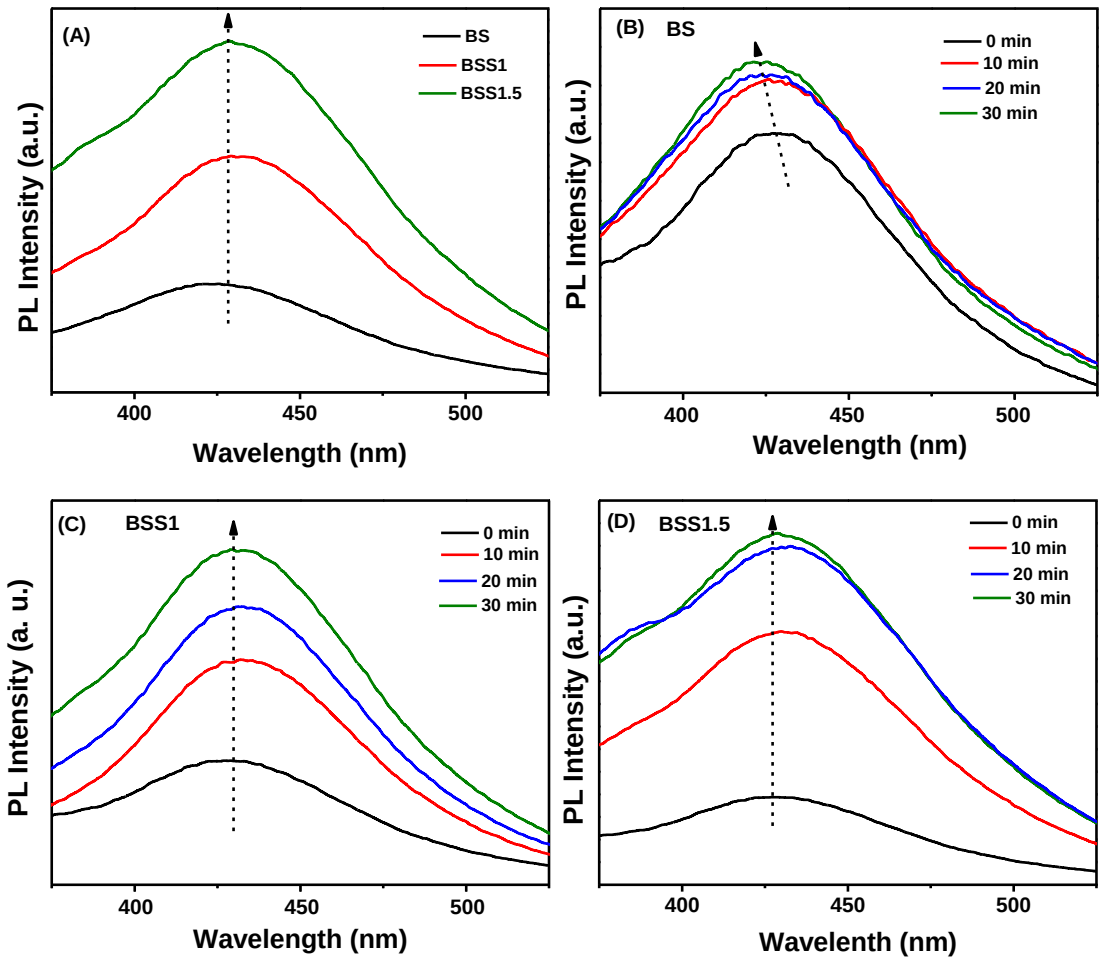

Fig. S11. (A) Determination of hydroxyl radicals on the surface of different photocatalysts under solar light irradiation for 30 min using photoluminescence spectra of TAOH (λ=315 nm) at 425 nm. Photoluminescence spectra of the solar light irradiated (B) BS, (C) BSS1, (D) BSS1.5 suspensions in terephthalic acid at different irradiation time.

Table S1: Relative band position of the Bi_2S_3 and SnS_2.

Semiconductor	**Electronegativity of the semiconductor (eV)**	**Optical band gap (eV)**	**Valance Band Position (eV)**		**Conduction Band Position (eV) (Experiment)**	
			Experiment	**Theory**	**Experiment**	**Theory**
Bi_2S_3	5.28	1.2	1.38	1.60	0.18	0.12
SnS_2	6.33	2.48	3.07	2.05	0.59	0.55

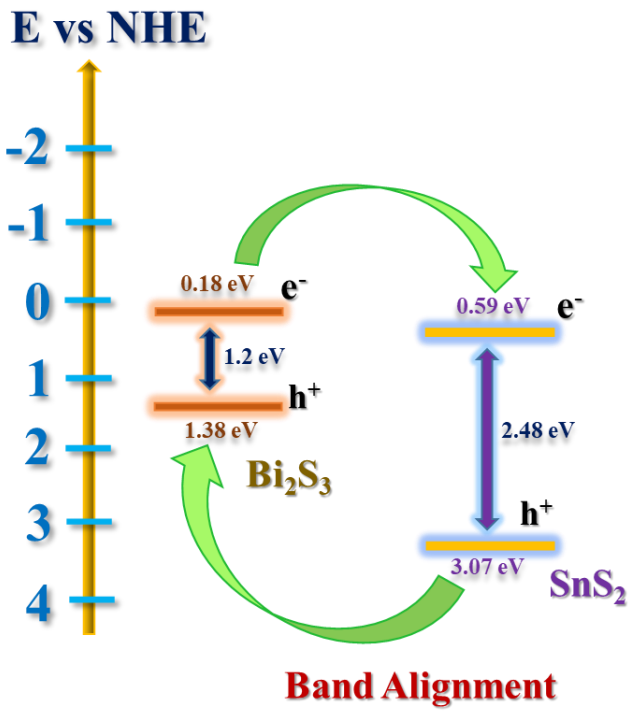

Scheme 1. Relative band alignment of Bi_2S_3 and SnS_2.